Journal of the Ceramic Society of Japan 118 [8] 674-678 2010 Paper

Characterization of barium titanate nanoparticles and dense nanograin free-standing films via sol–gel method using highly concentrated alkoxide solution

Hirokazu SHIMOOKA,† Shigemi KOHIKI and Makoto KUWABARA*

Department of Applied Chemistry, Kyushu Institute of Technology, 1–1 Sensui-cho, Tobata, Kitakyushu 804–8550
***Professor emeritus at the University of Tokyo, 4–36–501 Shimoshirouzukita, Kasuga, Fukuoka 816–0854**

This paper reports on two topics regarding nanosized barium titanate ($BaTiO_3$) prepared by the sol–gel method using a highly concentrated alkoxides precursor solution. One topic concerns the crystallographic features of the $BaTiO_3$ nanoparticles. In the case of using a highly concentrated precursor solution, non-core–shell $BaTiO_3$ nanocrystals with a small amount of intraparticle voids, lattice hydroxyl groups and remaining alkoxy groups were efficiently generated by the addition of less excess water during aging at room temperature. The generation of the high-quality $BaTiO_3$ nanocrystals is considered to be due to the hydrolysis and polycondensation reaction of the alkoxides being well promoted in such a concentrated solution. The lattice volume of the $BaTiO_3$ nanocrystals with a crystallite size of 15 nm fired at 600°C was approximately 1 vol % larger than that of bulk crystal. This lattice expansion is more likely to be caused by an intrinsic size effect than an extrinsic effect due to the lattice defects, such as lattice hydroxyl groups. The other topic concerns the dielectric properties of dense nanograin free-standing films with a grain size of 57 nm after applying the same sol–gel method. Significant frequency dispersion behavior of dissipation factor was observed at temperatures less than the Curie temperature. This finding may indicate that the dielectric properties reflect an intrinsic grain size effect without any influence being attributed to the film/substrate interface or lattice defects.

Key-words : Barium Titanate, Sol–gel method, Nanograin, Free-standing film, Dielectric property

[Received April 30, 2010; Accepted July 15, 2010]

1. Introduction

Barium titanate ($BaTiO_3$) ceramics are used as dielectric materials for multi-layer ceramic capacitors (MLCCs) due to their high permittivity.[1] To enable miniaturization of components and achieve higher capacitance and reliability, it is necessary to develop techniques to fabricate dense $BaTiO_3$ dielectric layers that consist of uniform nano-size grains less than several tens of nanometers in size. However, it is considered difficult to prepare such dielectric layers using traditional solid-state reaction methods without grain growth. For densification nanograin ceramics avoiding grain growth, many studies have been carried out using pressure-assisted sintering.[2] However, stress and strain often remain in such cases.

It is generally recognized that as the grain size is reduced to a few hundred nanometers, the permittivity at room temperature decreases.[3] However, the dielectric properties of nanograin $BaTiO_3$ ceramics with a grain size of less than 100 nm have not yet been clarified.[2),4] It is well known that the dielectric properties of $BaTiO_3$ are extremely sensitive to various factors such as stoichiometry, defects, impurities, electrical boundary conditions, stress and strain.[5)–8] Thus, establishing a novel fabrication method for the densification of nanograin $BaTiO_3$ ceramics without pressure is the key to resolving the issues concerning the dielectric properties in the size range of several tens of nanometers.

Fabrication of nanoparticles and densification of nanoparticles without grain growth are generally considered to be independent issues. However, in this study, we have focused on the sol–gel route as a unique method to simultaneously address both these issues. The sol–gel method can provide nano-size $BaTiO_3$ crystalline particles at lower temperatures.[9] In particular, if metal alkoxides are used as the starting materials, hydrolysis and polycondensation reaction occur easily and result in the formation of $BaTiO_3$ nanoparticles in the reaction container at low temperature as follows:

$$\begin{aligned} &Ba(OR)_2 + Ti(OR)_4 + 4H_2O \\ &\quad \rightarrow Ba^{2+} + 2OH^- + TiO_2\ (gel) + 6ROH \\ &\quad \rightarrow BaTiO_3 + H_2O + 6ROH \end{aligned} \tag{1}$$

where OR represents an alkoxy group.

The above equations show that increasing the precursor concentration effectively promotes the $BaTiO_3$ crystallization reaction. However, because many types of metal alkoxides exhibit low solubility in organic solvents, an excess of one or more of a reactant species of water, barium ions, or hydroxyl ions are needed to obtain crystalline $BaTiO_3$ nanoparticles.[10),11]

In contrast, we proposed an original approach to improve the solubility of metal alkoxides using mixed solvents.[12] In the case of methanol/2-methoxyethanol as the mixed solvent, a drastic increase in solubility was achieved when compared to cases in which each solvent was used individually. As a result, crystallization proceeded well without the addition of excess barium alkoxide and water, even at room temperature. Moreover, it should be noted that the crystallization mechanism appeared to be different from that in the dilute solution system. Specifically, it was found that there was a very small amount of dissolved barium species in the pore liquid within the gel framework, indicating that the mechanism was not based on a dissolution-

† Corresponding author: H. Shimooka; E-mail: shimooka@che.kyutech.ac.jp

precipitation scheme.[13] This hypothesis is also supported by evidence that Ostwald ripening did not occur after six months of aging at room temperature. We have already proposed a model to explain the crystallization mechanism based on a polycondensation reaction during aging. The most important point to be noted with regard to this model is the assumption that the stoichiometric corner-shared Ba–TiO_6 based clusters as a structural unit of the gel framework, which is indicated by extended X-ray absorption fine structure (EXAFS) and X-ray absorption near-edge structure (XANES) studies. Complete details of this model are provided in Ref. 14).

In the present study, we report on the crystallographic features of $BaTiO_3$ nanoparticles synthesized by the sol–gel method using a high-concentration metal alkoxides precursor solution. Then, on the basis of the same sol–gel method, fabrication of dense nanograin $BaTiO_3$ free-standing films are reported. Using the free-standing films as nanograin $BaTiO_3$ polycrystals, the effect of intrinsic size on the dielectric properties is examined.

2. Experimental procedure

Barium ethoxide and titanium isopropoxide were used as starting materials, and a mixture of methanol and 2-methoxyethanol in a volume ratio of 3:2 was used as the solvent. The use of this mixed solvent made it possible to dissolve a large amount of the alkoxides to produce a high-concentration precursor solutions of 1.2 mol/l at room temperature. The precursor solution was hydrolyzed with water vapor at 0°C with stirring for about 10 h so that the amount of water added to the precursor solution reached $H_2O/Ba \approx 5$–7 (molar ratio). The H_2O/Ba ratio at a certain point was estimated using a calibration curve, which was predetermined by the weight gain of the precursor solution. The sols were then aged in sealed containers at room temperature for several days. Next, the obtained wet gels were dried and then fired at 400–1000°C in oxygen after pulverizing using a mortar and pestle. Characterization of the crystallographic features of the gel-derived powders fired at various temperature was conducted using powder X-ray diffraction analysis (XRD; Rigaku, Geigerflex 2013), micro-Raman spectroscopy (Tokyo Instruments, Nanofinder30, Nd-YAG. 532 nm, 100 mW) and transmission electron microscopy (TEM; Hitachi, H-9000NAR, 300 kV).

Free-standing $BaTiO_3$ gel films were prepared at the nitrogen/liquid paraffin interface by spreading the pre-hydrolyzed high concentration precursor solution.[15] Pre-hydrolysis of the precursor solution was carried out by the addition of water vapor with an H_2O/Ba molar ratio of 2–3. The spreading requirement of liquid A on the surface of liquid B is to have a positive value of the spreading coefficient $S_{A/B}$ ($= \gamma_B - \gamma_A - \gamma_{AB}$), where γ_A and γ_B are the surface tension of liquids A and B, respectively, and γ_{AB} is the interface tension between liquids A and B. After gelation of the liquid films of pre-hydrolyzed precursor solution, the gel films were aged for several days at room temperature. The films were then dried and fired at a temperature range of 850–1200°C in an oxygen atmosphere. Nanograin $BaTiO_3$ free-standing films were characterized by micro-XRD (PANalytical, X'Pert PRO, Cu Kα) and field emission scanning electron microscopy (FE-SEM; JEOL, JSM-6320F). The temperature dependence of the dielectric properties of the free-standing films was measured using an impedance analyzer (YHP, 4192A) after applying an In-Ga liquid alloy to both sides of the films. The points where the alloy was applied acted as electrodes. The measurements were carried out at a cooling rate of 2°C/min with a measurement interval of 1°C.

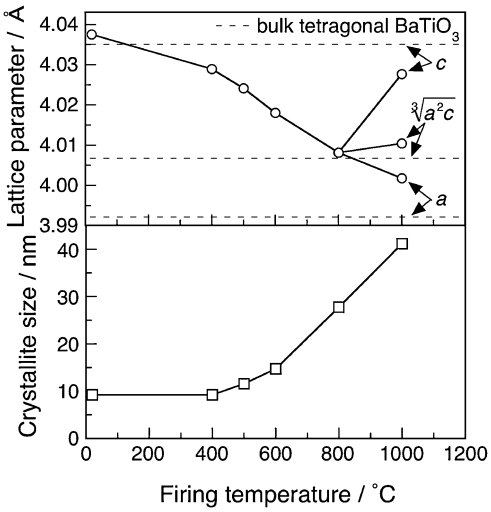

Fig. 1. Firing temperature dependence of lattice parameters and crystallite sizes of the gel-derived powders at room temperature.

3. Results and discussion

3.1 Crystallographic features of $BaTiO_3$ nanocrystals produced via sol–gel method using a highly-concentrated precursor solution

As previously reported, $BaTiO_3$ nanocrystals with a size of 10–20 nm generated in gels during aging were obtained at room temperature by the sol–gel method described above using a precursor concentration of 1.2 mol/l and an H_2O/Ba molar ratio of 5.5. The lattice parameters and crystallite sizes of the gel-derived powders formed at various firing temperatures are shown in **Fig. 1**. The results revealed that the lattice volume of gel-derived powders fired at temperatures lower than 800°C were larger than those of bulk tetragonal $BaTiO_3$. There are several possible reasons for this lattice volume expansion. One is the extrinsic effects attributed to lattice defects such as lattice hydroxyl groups[16] and any remaining alkoxy groups.[17] These effects vary depending on synthesis procedures. Another possible reason is an intrinsic effect attributed to the size of the crystalline particles. Tsunekawa et al.[18] reported that a $BaTiO_3$ lattice would expand in order to increase the ionicity of the Ti–O bond as their particle size decreased to less than about 15 nm. Perebeinosa et al.[19] pointed out that such expansion occurs as a result of the negative pressure created by the disconnection of the attractive Madelung potential of the small particles (< 20 nm approx.). Lattice hydroxyl groups, which are considered to be major defects in crystals produced via the sol–gel route, are known to burn out at temperatures of 500–600°C.[20] However, the lattice volume of samples with a crystallite size of 15 nm fired at 600°C was still approximately 1 vol % larger than that of bulk crystal. Hence, this lattice expansion is more likely to be caused by an intrinsic size effect than an extrinsic effect due to lattice defects such as lattice hydroxyl groups.

The crystal symmetries of $BaTiO_3$ nanocrystals fired at 600°C or higher, which were not influenced by extrinsic lattice defects such as hydroxyl groups, were characterized by XRD and micro-Raman analysis. XRD measurements revealed that the crystal symmetry of the samples fired below 800°C was cubic owing to the absence of splitting of the diffraction peaks of (200) and (002). However, it is not clear whether the absence of peak splitting was caused by true cubic symmetry consistent with that above the Curie temperature (T_c), or by line broadening due to

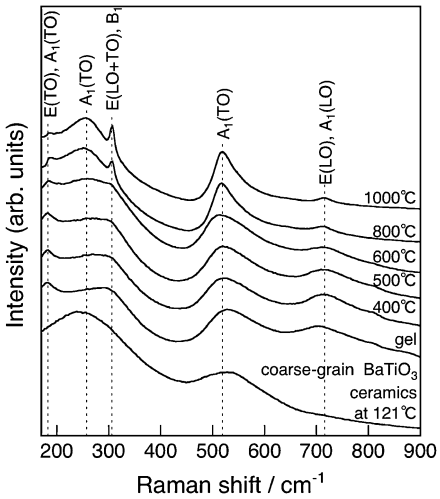

Fig. 2. Room temperature micro-Raman spectra of the gel-derived powders fired at various temperatures and spectrum of coarse-grain $BaTiO_3$ ceramics measured at 121°C.

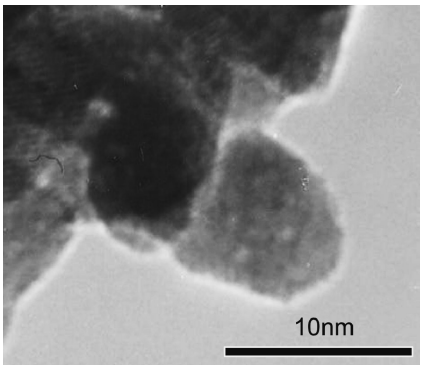

Fig. 3. TEM bright field image of the gel-derived powder fired at 400°C.

the small crystallite size. Thus, room temperature micro-Raman spectra of the gel-derived powders fired at various temperatures were measured to clarify the local and dynamic symmetry of the crystals, while XRD reflect the average and static symmetry of the crystals (**Fig. 2**). A relatively intense peak was observed at 305 cm^{-1} for samples fired at 800°C or higher. This peak was assigned to the E(LO + TO) mode of in-plane vibration (occurring in the xy plane) or to the B1 mode, which comprised only oxygen ion vibration in the xz and yz planes for the tetragonal $BaTiO_3$, because it is observed in the Y(XX)Y, X(ZY)X + ΔY, X(ZY)Z configuration.[21] Moreover, the other broad peaks around 180, 260, 520 and 720 cm^{-1} were consistent with coarse-grained tetragonal $BaTiO_3$.[22] Hence, the symmetry of $BaTiO_3$ nanoparticles fired at 800°C or higher are considered to be tetragonal. In contrast, the symmetry of the samples fired at 600°C or lower was not clear due to suppression of the peak at 305 cm^{-1}. However, because the features of the other broad peaks were similar to that of tetragonal $BaTiO_3$, the crystal structures of the samples fired at 600°C or less were also likely to be tetragonal rather than cubic (Fig. 2).

Next, the influence of the highly-concentrated precursor solution on the crystallographic features of $BaTiO_3$ nanoparticles is discussed below.

Many lattice hydroxyl groups are contained in the as-synthesized $BaTiO_3$ nanocrystals formed by the conventional sol–gel method. Hennings et al.[20] reported that lattice hydroxyl groups are released as water up to 500°C. The remaining oxygen vacancies and metal vacancies incorporated in the crystals then combine to form nanometer-sized intraparticle voids at 400°C or higher. In the case of $BaTiO_3$ particles produced by hydrothermal synthesis, these voids appear to grow by several tens of nanometers at around 500°C. Conversely, gel-derived powders fired at 400°C were found to have some small voids with sizes of 1–2 nm (**Fig. 3**). This result indicates that $BaTiO_3$ nanoparticles with few lattice hydroxyl groups can be obtained, suggesting that there is only a small amount of water or hydroxyl ions in the pore liquid within the gel matrix during the nucleation stage of $BaTiO_3$ crystals at room temperature. $BaTiO_3$ formation during aging is promoted efficiently without the addition of a large excess of water when highly-concentrated precursor solutions are used.[23),24] Crystallization of $BaTiO_3$ with few lattice hydroxyl groups is considered to be due to the requirement for only a small excess of water in such concentrated precursor solutions.

Reduction of the remaining alkoxy groups in the crystalline gels is also expected when highly-concentrated precursor solutions are used. In general, the remaining alkoxy groups burn in oxygen to form carbon dioxide and water vapor at temperatures below several hundred degrees centigrade. In the presence of carbon dioxide, thermodynamically stable barium carbonate and titania, or oxycarbonate $Ba_2Ti_2O_5CO_3CO_2$ are formed at comparatively low temperatures of up to 500°C.[25] However, in the case of gels derived from highly-concentrated precursor solutions, no intermediate species such as carbonate or oxycarbonate were detected after heat treatment at less than 600°C, despite there being a certain amount of amorphous gel frameworks in the as-synthesized gels.[26] Therefore, these results indicate that $BaTiO_3$, but not the thermodynamically stable carbonate, formed directly from the gel frameworks due to the similarity between the local symmetry of the amorphous gel and the $BaTiO_3$ crystals as well as the small amount of remaining alkoxy groups.[14),26] It appears that direct crystallization results in the formation of uniform tetragonal-like nanocrystals, but not core-shell particles[27] with a tetragonal core and a cubic shell.

3.2 Preparation of dense nanograin $BaTiO_3$ free-standing films and their dielectric properties

Because $BaTiO_3$ nanocrystals produced via the sol–gel method using highly-concentrated precursor solutions are considered to have good crystallographic properties, these crystals are expected to contribute to the progress in research concerning the intrinsic size effects of $BaTiO_3$ ceramics with a grain sizes of several tens of nanometers on dielectric properties, if the dense nanograin ceramics are obtained on the basis of this sol–gel method. In this study, preparation of dense nanograin $BaTiO_3$ ceramics in the form of free-standing films was attempted for the following reasons. One reason is to solve the problems concerning densification of the nanograin ceramics without grain growth at low temperatures. Nanoparticles generally tend to agglomerate to form large secondary particles, which lead to microstructural heterogeneity of the powder compacts and grain growth during sintering. However, as previously reported,[12] $BaTiO_3$ crystalline gels derived from highly-concentrated metal alkoxide precursor solutions show extremely good densification behavior without any pressure assistance or sintering aids. Even so, it is difficult to prepare dense $BaTiO_3$ ceramics with a grain size of less than 1 μm. On the other hand, free-standing $BaTiO_3$ gel films are densified at 1030°C to form ceramic films composed of grains less than 100 nm in size.[14] These results show that densification

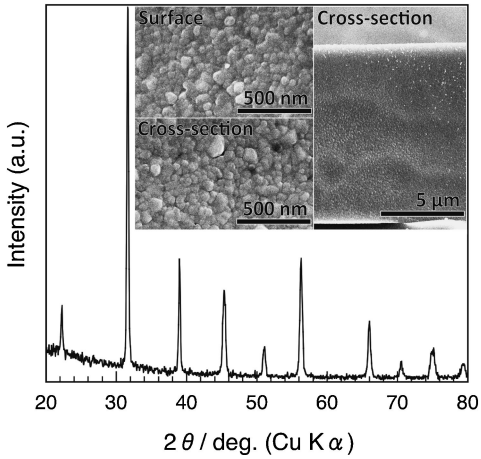

Fig. 4. Micro-XRD pattern of the $BaTiO_3$ free-standing film produced by two-step sintering technique[29] (first step at 900°C, second step at 850°C, in oxygen atmosphere). Inset: FE-SEM image of the film surface and cross-section.

of gels with a 2-dimensional film shape occurs easily and uniformly when compared to those with a 3-dimensional shape. This difference in densification behavior is considered to be due to the difference in the shrinking behavior of the gel framework by syneresis during aging.[28] Moreover, free-standing films can shrink in-plane during the densification process; however, ordinary films on substrates cannot shrink in-plane. The second reason is that the dense free-standing films were considered to be useful to clarify the dielectric properties attributed to the intrinsic size effects without any other factors, such as stress and strain due to differences in thermal expansion, and unfavorable chemical reactions at the film/substrate interfaces during heat treatment.

By applying a two-step sintering technique[29] (one step at 900°C, followed by a step at 850°C, in an oxygen atmosphere), a $BaTiO_3$ free-standing film with significantly dense nanograins and an average grain size of 57 nm was obtained, as shown in **Fig. 4**. The dielectric properties were measured using liquid alloy electrodes to prevent compressive or bending stress on the film. Because the liquid electrode/film interface might suffer from poor contacts because of the effect of surface roughness on the wettability, the electrode areas were not determined in this study. The thickness of the film used for this measurement was about 10.5 μm. The temperature dependence of the dielectric properties of the nanograin $BaTiO_3$ free-standing films are shown in **Fig. 5**a. For comparison, the properties of dense coarse grain free-standing films with a grain size of 1.6 μm sintered at 1200°C are also shown in Fig. 5b. It was confirmed that the coarse grain films show typical temperature dependence of the dielectric properties, similar to that of bulk $BaTiO_3$.[2] This result should ensure that the free-standing films can be used as high-quality bulk ceramics without remaining stress.

The capacitance of the film with a grain size of 57 nm was significantly flat for temperatures less than T_c. In addition, the capacitance appeared to almost fit the Curie–Weiss law in the temperature range of T_c–200°C. It should be noted that T_c was clearly observed to be at 115°C; this value was slightly lower than that of the T_c of coarse grain $BaTiO_3$, despite the fact that most of $BaTiO_3$ films on substrates that have been reported to date had broad temperature dependence of permittivity and unclear T_c. These effects of conventional $BaTiO_3$ films on substrates are reported to be extrinsic, and caused by surface

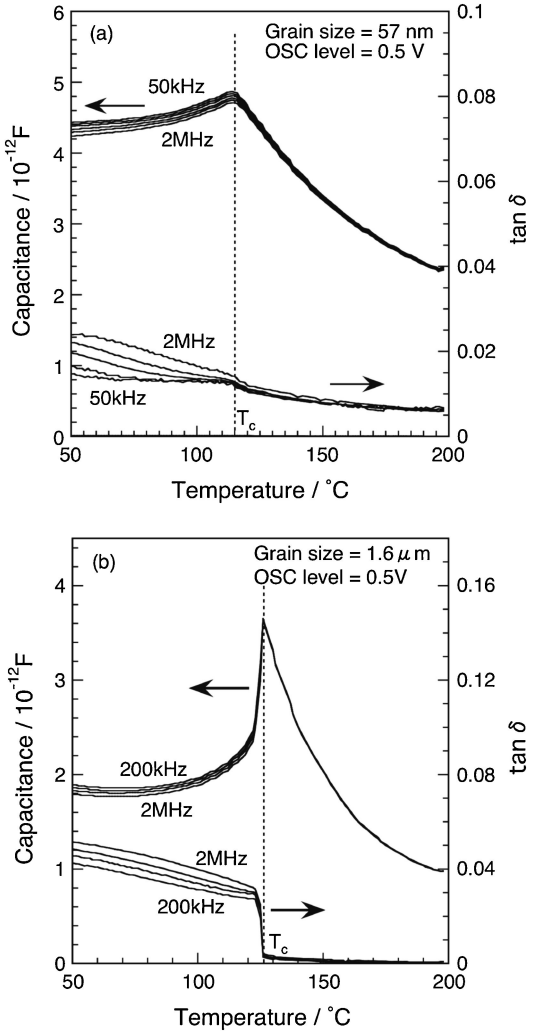

Fig. 5. Temperature dependences of capacitance and dissipation factor for $BaTiO_3$ free-standing films with an average grain size of (a) 57 nm and (b) 1.6 μm.

effect.[30] Moreover, significant frequency dispersion behavior of tan δ was observed at temperatures less than T_c. These findings may indicate that the dielectric properties reflect intrinsic grain size effects without any problems attributed to the film/substrate interface. This remarkable frequency dispersion will be discussed in a future publication.

4. Conclusion

The major conclusions of this study can be summarized as follows:

Hydrolysis and polycondensation reactions were efficiently promoted by using a highly-concentrated precursor solution, resulting in the formation of non-core–shell $BaTiO_3$ nanocrystals with few intraparticle voids, attributed to the small amount of lattice hydroxyl groups and remaining alkoxy groups.

The lattice volume of the $BaTiO_3$ nanocrystals with a crystallite size of 15 nm was approximately 1 vol % larger than that of bulk crystal.

The crystal structures of the $BaTiO_3$ nanocrystals with a crystallite size of 15 nm also appeared to be tetragonal and not cubic.

Dense nanograin $BaTiO_3$ free-standing films with a grain size of 57 nm were obtained by applying the same sol–gel method using highly-concentrated precursor solution.

The capacitance of the film with a grain size of 57 nm was significantly flat over temperatures less than T_c. T_c was clearly observed at 115°C.

Significant frequency dispersion behavior of dissipation factor was observed at temperatures less than T_c.

Acknowledgments The authors wish to thank Fukuoka Industrial Technology Center for the use of their micro-XRD equipment.

References

1) H. Kishi, Y. Mizuno and H. Chazono, *Jpn. J. Appl. Phys.*, 42, 1–15 (2003).
2) M. H. Frey, Z. Xu, P. Han and D. A. Payne, *Ferroelectrics*, 206–207, 337–353 (1998).
3) G. Arlt, D. Hennings and G. de With, *J. Appl. Phys.*, 58, 1619–1625 (1985).
4) X. Wang, X. Deng, H. Wen and L. Li, *Appl. Phys. Lett.*, 89, 162902 (2006).
5) S. Lee, Z.-K. Liu, M.-H. Kim and C. A. Randall, *J. Appl. Phys.*, 101, 054119 (2007).
6) M. Stengel and N. A. Spaldin, *Nature*, 443, 679–682 (2006).
7) G. Arlt and N. A. Pertsev, *J. Appl. Phys.*, 70, 2283–2289 (1991).
8) N. Wada, H. Tanaka, Y. Hamaji and Y. Sakabe, *Jpn. J. Appl. Phys.*, 35, 5141–5144 (1996).
9) K. S. Mazdiyasni, R. T. Dolloff and J. S. Smith, II, *J. Am. Ceram. Soc.*, 52, 523–526 (1969).
10) M. I. Diaz-Guemes, T. G. Carreno, C. J. Serna and J. M. Palacios, *J. Mater. Sci.*, 24, 1011–1014 (1989).
11) M. H. Frey and D. A. Payne, *Chem. Mater.*, 7, 123–129 (1995).
12) H. Shimooka and M. Kuwabara, *J. Am. Ceram. Soc.*, 78, 2849–2852 (1995).
13) H. Shimooka and M. Kuwabara, *J. Am. Ceram. Soc.*, 79, 2983–2985 (1996).
14) H. Shimooka and M. Kuwabara, *J. Ceram. Soc. Japan*, 105, 811–814 (1997).
15) H. Shimooka, T. Yamamoto, S. Takahashi and S. Kohiki, *J. Sol-Gel Sci. Technol.*, 19, 749–752 (2000).
16) T. Noma, S. Wada, M. Yano and T. Suzuki, *J. Appl. Phys.*, 80, 5223–5233 (1996).
17) C. Miot, E. Husson, C. Proust, R. Erre and J. P. Coutures, *J. Mater. Res.*, 12, 2388–2392 (1997).
18) S. Tsunekawa, S. Ito, T. Mori, K. Ishikawa, Z.-Q. Li and Y. Kawazoe, *Phys. Rev. B*, 62, 3065–3070 (2000).
19) V. Perebeinosa, S.-W. Chan and F. Zhang, *Solid State Commun.*, 123, 295–297 (2002).
20) D. F. K. Hennings, C. Metzmacher and B. S. Schreinemacher, *J. Am. Ceram. Soc.*, 84, 179–182 (2001).
21) A. Scalabrin, A. S. Chaves, D. S. Shim and S. P. S. Porto, *Phys. Status Solidi B*, 79, 731–742 (1977).
22) L. H. Robins, D. L. Kaiser, L. D. Rotter, P. K. Schenck, G. T. Stauf and D. Rytz, *J. Appl. Phys.*, 76, 7487–7498 (1994).
23) S. Takahashi, H. Ohmura, K. Miki, H. Shimooka and M. Kuwabara, *J. Ceram. Soc. Japan*, 102, 1182–1184 (1994).
24) H. Shimooka, K. Yamada, S. Takahashi and M. Kuwabara, *J. Sol-Gel Sci. Technol.*, 13, 873–876 (1998).
25) S. Kumar, G. L. Messing and W. B. White, *J. Am. Ceram. Soc.*, 76, 617–624 (1993).
26) H. Shimooka and S. Kohiki, *J. Ceram. Soc. Japan*, 106, 703–708 (1998).
27) S. Wada, T. Hoshina, K. Takizawa, M. Ohishi, H. Yasuno, H. Kakemoto, T. Tsurumi, C. Moriyoshi and Y. Kuroiwa, *J. Korean Phys. Soc.*, 51, 878–881 (2007).
28) C. J. Brinker and G. W. Scherer, "Sol-Gel Science: The Physics and Chemistry of Sol-Gel Processing," Academic Press, Boston (1990) pp. 441–444.
29) I.-W. Chen and X.-H. Wang, *Nature*, 404, 168–171 (2000).
30) A. M. Bratkovsky and A. P. Levanyuk, *Phys. Rev. Lett.*, 94, 107601 (2005).